Necessity and adequacy of near-source factors for seismically isolated buildings

Muhammad Khalid Saifullah[a] and Cenk Alhan*

Department of Civil Engineering, Istanbul University, 34320 Avcılar, Istanbul, Turkey

Abstract. Superstructures and isolation systems of seismically isolated buildings located close to active faults may observe increased seismic demands resulting from long-period and high-amplitude velocity and displacement pulses existent in near-fault ground motions as their fundamental periods may be close to or coincident with these near-fault pulse periods. In order to take these effects into account, the 1997 Uniform Building Code (UBC97) has specified near-source factors that scale up the design spectrum depending on the closest distance to the fault, the soil type at the site, and the properties of the seismic source. Although UBC97 has been superseded by the 2015 International Building Code in the U.S.A., UBC97 near-source factors are still frequently referred in the design of seismically isolated buildings around the world. Therefore it is deemed necessary and thus set as the aim of this study to assess the necessity and the adequacy of near-source factors for seismically isolated buildings. Benchmark buildings of different heights with isolation systems of different properties are used in comparing seismic responses obtained via time history analyses using a large number of historical earthquakes with those obtained from spectral analyses using the amplified spectrums established through UBC97 near-source factors. Results show that near-source factors are necessary but inadequate for superstructure responses and somewhat unconservative for base displacement response.

Keywords: near-source factors; seismically isolated buildings; time history analysis; response spectrum analysis

1. Introduction

Every day, we experience many types of natural hazards in different parts of the world but earthquakes are the ones with considerably greater damage potential resulting in severe social and economic impact. Many times economic losses are so significant that it takes decades for some countries to gain economic revival. And a more serious concern is the loss of lives during these extreme events. According to a rough estimate, every year earthquakes take the lives of 20000 people on average (Tsang *et al.* 2012). As it is impossible to anticipate the exact location, timing, and/or magnitude of these events, engineers rather focus on designing earthquake resistant structures. The traditional approach to seismic hazard mitigation is to design a structure that has sufficient strength capacity and the ability to deform in a ductile manner. On the other hand, innovative concepts of structural control have been increasing in recognition and may obviate the necessity of inelastic deformation allowance in the structures (Symans and Constantinou 1999, Martelli *et al.* 2014, Dan *et al.* 2015). Passive control systems are the most widely used ones at the moment which have considerable cost advantage over active and semi-active ones. And seismic isolation is a type of passive control system which usually employs elastomeric bearings or frictional sliding mechanisms as isolation system elements which are typically introduced between the foundation and the superstructure. This laterally flexible isolation system lengthens the fundamental period of the structure and thus detunes it from the high dominant frequencies of the earthquake while energy is absorbed through the damping mechanism existent in the isolation system thereby reducing superstructure responses like floor accelerations and inter-story drifts and thus preventing injuries to the occupants while keeping the structure intact (Alhan *et al.* 2006, Gavin *et al.* 2003).

Owing to its proven success under strong ground motions with typical high frequency content, seismic isolation is being implemented with an ever increasing rate around the world (Martelli *et al.* 2014) and with more than 6000 seismically isolated buildings or houses; Japan leads the way in seismic isolation (Kani 2011). However, ground motion records obtained at stations close to the faults, typically within 15 km from the fault testify the fact that near-fault ground motions may contain strong, large-amplitude, and in particular long-period velocity and displacement pulses (Hoseini Vaez *et al.* 2014). The pulses existent in near-fault ground motions may appear as single or double pulses with single or double sided amplitudes (Bolt 2004) that can arise due to the directivity effects and/or fling step motion (Bolt and Abrahamson 2003). The periods of these pulses typically range from 0.5 to 5 seconds (Bolt 2004) and such long-period pulses may threaten seismically isolated structures with long fundamental periods (Heaton *et al.* 1995, Hall *et al.* 1995, Hall and Ryan 2000, Alhan and Gavin 2004, Mazza and Vulcano 2009, Alhan and Öncü-Davas 2016).

A study by Heaton *et al.* (1995) suggests that a

---

*Corresponding author, Associate Professor
 E-mail: cenkalhan@istanbul.edu.tr
[a]Former Graduate Student

seismically base isolated building subjected to a near-fault M_w 7.0 blind thrust earthquake excitation, even if damped at 25% of critical damping, could undergo large isolator displacements in excess of 0.5 m. These unwanted and enormous isolator drifts can result in buckling and/or tearing of the isolator. And the criticality of the isolation system can be understood from the fact that the integrity of the seismically isolated building is dependent upon the isolation system which is highly determinate and lacks alternate load transfer paths. Realizing this fact, researchers have focused on providing means to reduce such large base displacement demands. Hybrid base isolation that makes use of passive viscous dampers along with isolators dates back to early 1990s. The study of application of fluid viscous dampers in buildings and bridges to improve seismic performance began in 1991 with Taylor Devices (a supplier to U.S. Government of dampers and shock absorbers) teaming up with State University of New York at Buffalo (Taylor 1996). Constantinou and Symans (1992) through experimental testing studied the behavior of 1 story and 3 story steel frame building models incorporating fluid viscous dampers and concluded that they offer a considerable reduction in story drifts as well as story shears. And, the first application of passive viscous dampers in forming a hybrid base isolation system of a full scale civil engineering structure was on five buildings of the San Bernardino County Medical Center Replacement Project. Passive viscous dampers had to be used in this project since use of only high damping rubber bearings resulted in unacceptably large base displacements under near-fault ground motions (Asher *et al.* 1996, Taylor 1996). Later, Hussain *et al.* (1998) investigated the effect of addition of linear viscous dampers to conventional base-isolated structures by using two-story building model and showed how forming hybrid base isolation by adding viscous dampers to flat sliding, friction pendulum and elastomeric isolation systems improve performances of these systems. Makris and Chang (2000) conducted research on 1 DOF and 2 DOF seismically isolated structures under cycloidal pulses and concluded that for structures with isolation period of 3 s, a combination of friction and viscous damping provides an attractive solution in limiting base displacements. In more recent studies, through shaking table testing of a seismically isolated building, Lu *et al.* (2013) noted that the isolation system can undergo resonance like behavior when excited by a pulse-like excitation that has a pulse period close to the isolation period and suggested that viscous dampers installed within the isolation layer can effectively reduce the large isolator displacements that may be realized due to such resonance like behavior and the effect of viscous damping on the response of a seismically isolated structure was studied by Wolff *et al.* (2015) who reported that viscous dampers, whether linear or nonlinear, can effectively reduce isolator displacements. On the other hand, it was also pointed out in previous studies that although use of higher damping can effectively reduce isolator displacements they can increase higher mode responses and thus cause amplifications in the superstructure responses such as floor accelerations and inter-story drifts, defeating the very purpose of seismic

isolation (Kelly 1999, Jangid and Kelly 2001, Alhan and Gavin 2004, Providakis 2008, Providakis 2009, Mazza and Vulcano 2009, Alhan C and Öncü-Davas 2016).

In order to avoid amplification in the roof accelerations, different types of devices other than viscous dampers are also proposed to form hybrid isolation systems. For example, passive variable friction damper, in which damping force is proportional to friction force that varies as a function of displacement Ribakov *et al.* (2006), was shown to significantly reduce base displacements of a seismic isolation system with these dampers and at the same time provide a similar performance to an optimally controlled case in terms of roof acceleration (Ribakov 2010). In another study, Ribakov and Agranovich (2008a) have shown that the addition of passive friction dampers, whose properties were selected such that the seismic responses of a base isolated building with these dampers would be close to that of a building equipped with active damping devices that are optimally controlled, would reduce base displacements (up to 25%) without increasing floor accelerations. Ribakov and Iskhakov (2008) also suggested that hybrid isolation systems incorporating variable friction dampers could be used to limit base displacements and obtain enhanced structural response particularly for public buildings which require higher safety level compared to residential ones. Various types of active and semi-active dampers have also been suggested by researchers as an effective solution in reducing base displacement without significantly increasing superstructure response. As a representative example of the earlier studies, Inaudi and Kelly (1993) worked on a hybrid isolation system incorporating laminated rubber bearings and actively controllable viscodampers and demonstrated the superiority of this active isolation system over passive systems in reducing floor accelerations. But, potential stability problems, high device force requirements and cost associated with active isolation systems hindered its widespread use in practice. On the other hand, as shown by Ramallo *et al.* (2002), base-isolated structures with semi-active smart dampers can significantly reduce base drifts along with structural accelerations, structural drifts and base shear as compared to those with passive isolation systems. Different types of semi-active dampers including variable stiffness dampers, hydraulic dampers, friction dampers, magnetorheological dampers, electrorheological dampers, variable friction dampers with piezoelectric actuators, etc. are developed aiming to reduce base displacements without significantly increasing the superstructure responses (Ribakov 2011). Makris (1997) studied the influence of semi-active electrorheological dampers in base-isolated structures to tackle long period ground motions and demonstrated that inclusion of such devices can substantially reduce displacement of the isolation system while keeping base shear at low levels. A five-story hybrid base-isolated building employing low damping rubber bearings in conjunction with passive viscous dampers, resetting semi-active stiffness dampers and semi-active electromagnetic friction dampers, and combination of the aforementioned passive and semi-active dampers, respectively, have been investigated by Yang and Agarwal

(2002) under near-fault ground motions. They concluded that these hybrid isolation systems perform well as compared to base-isolated building alone under near-field earthquakes. Gavin *et al.* (2003) numerically studied the response of a six-story building equipped with lead rubber bearings and semi-active hydraulic dampers and came up with the conclusion that under pulse-type ground motions this type of system performs better than conventional base-isolated system. Nitta *et al.* (2006) proposed a scheme in which the slip-force levels of the magnetorheological damper are controlled based on the measurement of absolute acceleration and damping forces and concluded that this type of semi-active mechanism when introduced into base-isolated structures results in reduction in both base shear and structural shear level. Although hybrid isolation systems employing passive viscous dampers or semi-active dampers may provide an effective solution in reducing base displacements without significantly increasing superstructure responses as discussed above, currently passive viscous dampers are used in many seismic isolation projects around the world. And, high passive supplemental viscous damping should not be used unless it is absolutely necessary, which consequently means that accurate prediction of base displacement demands particularly under near-fault earthquakes is a vital issue. Furthermore, regardless of the damping level, pulse-like near-fault earthquakes may cause much larger superstructure responses in seismically isolated buildings compared to those caused by typical far-fault earthquakes, which must also be accurately predicted from a performance-based design point of view.

In order to take the aforementioned effects of near-fault earthquakes into account, Uniform Building Code (1997) has specified near-source factors, both for conventional fixed-base and seismically isolated buildings, which scale up the earthquake design spectrum depending on the closest distance from the fault, the soil type, and the seismic source type. In a study conducted by Hall and Ryan (2000), a six-story base isolated building designed in compliance with the UBC97, using the near-source factors, showed elastic behavior when subjected to actual near-fault ground motion records. But it was also shown that building responses may be pushed well into the nonlinear range if the building is subjected to either a hypothetical Mw=7.0 blind thrust earthquake or the most severe motion from the 1994 Northridge Earthquake. And recently, Alhan and Sürmeli (2015) investigated the adequacy and necessity of UBC97 near-source factors for conventional fixed-base buildings and concluded that these factors are utterly necessary but the current values are inadequate for fixed-base buildings. It should be noted here that although UBC97 has been superseded by the 2015 International Building Code in the U.S.A., which makes use of detailed spectral maps instead of near-source factors, UBC97 near-source factors are still frequently used in practical design work around the world. The designs of seismically isolated buildings, in the countries with seismic codes that do not contain detailed spectral maps, are carried out by making use of UBC97 near-source factors which conveniently employ closest fault-distance, fault-type and earthquake magnitude

information. According to authors' knowledge, for example countries including Pakistan (Building Code of Pakistan - Seismic Provisions 2007), India (Indian Standard - Criteria for Earthquake Resistant Design of Structures 2002) and Iran (Iranian Code of Practice for Seismic Resistant Design of Buildings 2007) make use of seismic zones rather than detailed spectral maps. Likewise, seismic zones, as opposed to detailed spectral maps, are used in most countries in Central and South America, which are known for their high seismicity (Chavez 2012). Seismically isolated buildings to be constructed in such areas would require the use of UBC97 near-source factors as their building codes are based on seismic zone mapping.

2. Aim, scope, and limitations

As discussed above, near-fault ground motions containing long period velocity and displacement pulses can bring about the wearing and/or tearing of isolators as the displacement demands become excessively large and thus raising a serious concern about the safety of seismically isolated buildings. A recent paper co-authored by the second author of this study (Alhan and Öncü-Davas 2016) revealed the performance limits of seismically isolated buildings under near-fault earthquakes. Base displacement and top floor acceleration demands of buildings equipped with different isolation systems of different characteristic parameters were obtained under synthetically developed near-fault ground motions at different fault distances with different velocity pulse periods. Then, the demands were compared to current practical and economical limits. It was concluded that the protection of vibration sensitive equipment, under large magnitude pulse-like near-fault ground motions, is a highly challenging task for seismically isolated buildings and that ratio of isolation period to pulse period significantly affects the peak floor acceleration and peak base displacement demands in case of short and long pulse periods, respectively.

It is a common practice among practicing engineers to use linear response spectrum analysis. And, near-source factors as found in UBC are intended to incorporate the aforementioned near-fault effects in the response spectrum. These near-source factors are not only used in the seismic analysis of seismically isolated buildings but also for conventional fixed-base buildings. Considering the significance of these factors, recently, Alhan and Sürmeli (2015) investigated the adequacy and necessity of these factors for ordinary fixed-base buildings by employing 3, 8 and 15-story benchmark buildings. In order to demonstrate the necessity of these factors, they made use of spectrums established through Turkish Earthquake Code (TEC07) which does not contain near-source factors and UBC97 which does employ near-source factors and compared the spectral responses with those of time-history analyses conducted under near-fault earthquakes. They concluded that near-source factors are necessary for the safe design of conventional fixed-base buildings in the vicinity of faults and mentioned the inadequacy of these factors for certain fault distances. Given the fact that these factors have been

proved quite necessary but inadequate for fixed-base buildings, it impelled the authors to investigate the adequacy and necessity of these factors for seismically isolated buildings. To the best of authors' knowledge, research which tests the adequacy and the necessity of near-source factors for seismically isolated buildings by making use of a wide historical ground motion data base does not exist in the literature.

The aim of this study is to assess the adequacy and necessity of the near-source factors specified in UBC97 for seismically isolated buildings. To this end, the seismic responses of benchmark seismically isolated buildings obtained via time history analyses using a large number of historical earthquakes are compared with those obtained from spectral analyses that make use of the amplified spectrums established using UBC97 near-source factors. The comprehensive parametric analyses conducted herein employ different types of isolation systems with different isolation system characteristic strengths and isolation periods, soil types A to E, and seismic source types A and B. Superstructure flexibility is also taken into account by including buildings with 3 and 8 stories. The benchmark buildings are subjected to a total of 110 historical earthquake records, each with two components, within 15 km vicinity of the fault lines, which is a compatible range with the range of closest fault-distances considered in UBC97.

It should be noted here that most seismically isolated buildings in the world are low to mid-rise but application of seismic base isolation to high-rise buildings and related research is also gaining popularity recently. It was reported by Naderzadeh (2009) that 12-story seismically isolated residential buildings were being constructed in Iran with the help of Malaysian developers as of 2009. Recently, Lu and Panagiatou (2015) studied the response of a 20-story building with dual-isolation system, which makes use of isolation plane at the base of the building with a post-tensioned rocking core wall, under near-fault earthquakes and concluded that this type of system shows excellent damage-resistant behavior under near-fault earthquakes. Becker et al. (2015) studied the response of a 32-story seismically isolated building and concluded that peak story drifts and peak floor accelerations in the superstructure decreased as a result of isolation. Thus, it would be beneficial to investigate the adequacy of near-source factors for high-rise seismically isolated buildings as part of a future study, however, we have excluded this class of buildings in the current study since the design of high-rise buildings with seismic isolation needs special consideration of problems like stability of large-size rubber bearings under tensile loading or uplift as stated by Komuro et al. (2005). In case of high-rise buildings with large height-to-width aspect ratios, tension forces may become excessive and result in rupture or uplift of bearings thus requiring special tension-resistant isolation bearings (Lu et al. 2016). These special design requirements are not a concern in typical low to mid-rise seismically isolated buildings which encompasses most of the practical ranges of seismically isolated buildings and have been covered in this study. Other assumptions and limitations of this study include the

following: The isolation system and the superstructure are both assumed to be symmetric. The superstructure is assumed to behave linearly elastic in seismic analyses. Soil-structure interaction and the influence of vertical earthquake excitation are not taken into consideration.

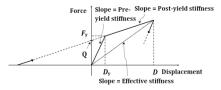## 3. Nonlinear hysteretic and equivalent linear models for seismic isolation

The isolation systems are represented by nonlinear hysteretic models in nonlinear time history analyses and by equivalent linear models in linear spectrum analyses. The parameters that define isolation systems composed of high damping rubber bearings (HDRB) or lead rubber bearings (LRB) exhibiting nonlinear hysteretic behavior and those used to define the equivalent linear ones are described in this section. The real nonlinear hysteretic behavior of elastomeric isolation systems that are composed of HDRBs or LRBs can be conveniently represented by the bilinear hysteretic force-deformation relationship shown in Fig. 1. Yield force (F_y) is the point on the hysteretic model at which pre-yield or initial stiffness (K_1) changes to post-yield or secondary stiffness (K_2) with the displacement attained until this point is called yield displacement (D_y). In reality, it is not a point but idealized as a point in truly bilinear models as opposed to smooth bilinear models where the transition from pre-yield to post-yield stage is smooth. Characteristic force or strength (Q) is the point at which the hysteretic curve intercepts the force axis as shown in Fig. 1. Post-yield to pre-yield stiffness (α) is another important parameter used to represent the difference between post and pre-yield stiffness. Important relationships between the aforementioned parameters can be derived from the geometry of the shape given in Fig. 1 as follows (Naeim and Kelly 1999)
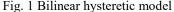
$$Q = (K_1 - K_2)D_y \qquad (1)$$

$$K_1 = \frac{F_y}{D_y} \qquad (2)$$

$$\alpha = \frac{K_2}{K_1} \qquad (3)$$

Nonlinear hysteretic isolation systems can be modeled as equivalent linear systems by employing "effective parameters", which is discussed at length by Matsagar and Jangid (2004) and Alhan and Özgür (2015): Effective stiffness (K_{eff}) is also known as the secant stiffness, which is defined at a given base displacement (D). Effective damping (β_{eff}) is the equivalent viscous damping, as percentage of critical, of a nonlinear isolation system modeled linearly, which is also defined at a given base

Fig. 1 Bilinear hysteretic model

displacement (D). For example, this base displacement (D) can be the code prescribed design displacement (D_D) or maximum displacement (D_M), depending on the level of seismic ground motion, as exemplified in Section 5.

By making use of the geometry in Fig. 1, following relationship for effective stiffness (K_{eff}) is obtained as

$$K_{eff} = K_2 - \frac{K_2 D_y - F_y}{D} = K_2 + \frac{Q}{D} \qquad (4)$$

And effective damping ratio (β_{eff}) with the corresponding effective damping coefficient (C_{eff}) is given by

$$\beta_{eff} = \frac{4Q(D - D_y)}{2\pi K_{eff} D^2} \qquad (5)$$

$$C_{eff} = \frac{4\beta_{eff} M\pi}{T_{eff}} \qquad (6)$$

For linear isolation systems, the fundamental period is calculated based on the effective stiffness (K_{eff}) and called effective isolation period (T_{eff}). On the other hand, since there exists two stiffnesses in nonlinear isolation systems, the pro-longed period associated with the isolated mode or the rigid-body-mode is commonly calculated based on the post-yield stiffness (K_2) and called the isolation period (T_b)

$$T_{eff} = 2\pi \sqrt{\frac{M}{K_{eff}}} \qquad (7)$$

$$T_b = 2\pi \sqrt{\frac{M}{K_2}} \qquad (8)$$

Where, M is the total mass of the building including the base supported by the isolation system (Nagarajaiah *et al.* 1991).

4. Isolation system displacements and seismic coefficients employing near-source factors

Per UBC97, design displacement (D_D), given by Eq. (9), is the minimum lateral earthquake displacement which the isolation system must be designed for. It is calculated in the directions of main horizontal axes of the structure and obtained for design basis earthquake (DBE) which is defined as the level of seismic ground motion that has a 10 percent probability of being exceeded in a 50 year period. It is important from the perspective that gaps to be left on either side of the building are based on these displacements. Apart from that, it is also worth-mentioning that the structural base shear associated with this displacement level is considered for the design of the superstructure

$$D_D = \frac{\left(\frac{g}{4\pi^2}\right) C_{VD} T_D}{B_D} \qquad (9)$$

Here, the effective stiffness is obtained at design displacement D_D via Eq. (4) which is then placed in Eq. (7) in order to obtain T_D, the effective period at design displacement D_D. The other parameters are the gravitational acceleration, g, the seismic coefficient, C_{VD}, and the numerical reduction coefficient B_D that is obtained from tables in UBC97 corresponding to the effective damping

ratio of the isolation system calculated at design displacement D_D via Eq. (5).

Maximum displacement (D_M), given by Eq. (10), is the maximum displacement of the isolation system in the most critical direction of the horizontal response that must be endured by the elements of the isolation system. It is based on the maximum capable earthquake (MCE) loading which is defined as the level of earthquake ground motion that has a 10 percent probability of exceedance in a period of 100 years. As mentioned earlier, the integrity of the whole superstructure relies on the isolation system which itself is highly determinate and lacks extra/alternate load transfer paths. Keeping in view this criticality of the isolation system, it has to be designed to withstand the maximum level of lateral displacements associated with MCE

$$D_M = \frac{\left(\frac{g}{4\pi^2}\right) C_{VM} T_M}{B_M} \qquad (10)$$

Here, the effective stiffness is obtained at maximum displacement D_M via Eq. (4) which is then placed in Eq. (7) in order to obtain T_M, the effective period at maximum displacement D_M. The other parameters are the gravitational acceleration, g, the seismic coefficient C_{VM}, and the numerical reduction coefficient B_M that is obtained from tables in UBC97 corresponding to the effective damping ratio of the isolation system calculated at maximum displacement D_M via Eq. (5).

As discussed in Introduction Section, the regions which are under the threat of large magnitude earthquakes and are located within the vicinity of the fault lines would experience much larger ground accelerations than distant regions. Furthermore, these near-fault regions may face long period ground velocity and displacement pulses, which would have a very negative impact particularly on long-period structures like seismically isolated buildings. Near-source factors take these issues into account and instill the implications to the aforementioned seismic coefficients (C_{AD}, C_{AM}, C_{VD}, and C_{VM}). There are two types of near-source factors defined in UBC 97. N_a is the acceleration-based near-source factor which is important for short-period structures while N_v is the velocity-based near-source factor which is vital for the long-period structures. The values of N_a and N_v for different seismic source types and various closest fault distances (r) are given in Table 1. Note that seismic source type is mainly based on the capability of the fault to produce large magnitude earthquakes. Faults that are capable of producing large magnitude earthquakes ($M_w \geq 7$) are considered as seismic source type A (SSTA). Faults that are not capable of producing large magnitude earthquakes (i.e., $M_w \leq 6.5$) and have relatively low rate of seismic activity are considered as seismic source type C (SSTC). Seismic source type B (SSTB) constitutes faults which are neither type A nor type C and can produce earthquakes of magnitudes between 6.5 and 7.0. Slip rate of fault is another important parameter in classifying the seismic sources (UBC97 1997).

The values of seismic coefficients directly depend on the near-source factors described above. They are very important as they are used for the construction of design spectra over which linear response spectrum analyses

Table 1 Near-source factors (UBC 97)

	N_a			N_v			
Seismic Source Type (SST)	r≤2 km	r=5 km	r≥10 km	r≤2 km	r=5 km	r=10 km	r≥15 km
A	1.5	1.2	1	2	1.6	1.2	1
B	1.3	1	1	1.6	1.2	1	1
C	1	1	1	1	1	1	1

are performed and also to calculate the design and maximum displacements given in Eqs. (9) and (10), respectively. Seismic coefficients C_{AD} and C_{AM} are the acceleration dependent coefficients used to create design response spectrum at a loading level of design basis earthquake and maximum capable earthquake, respectively. C_{VD} and C_{VM} are the velocity dependent seismic coefficients used to create design response spectrum at a loading level of design basis earthquake and maximum capable earthquake, respectively. C_{AD} and C_{AM} are associated with N_a while C_{VD} and C_{VM} are associated with N_v. The values of seismic coefficients also change with the type of soil under consideration. Soil profile types are mainly based on the shear wave velocity of the soil. Per UBC97, the soils with very high shear wave velocity

($\bar{v}_s$ >1500 m/s) are classified as A type soils while those with low shear wave velocity ($\bar{v}_s$ <180 m/s) are considered as E type soils. F type soils are considered as the ones requiring site specific evaluation.

Seismic coefficients which are calculated for r=2, 5, 10, and 15 km and soil types A, B, C, and D are presented in graphical form in Fig. 2, which have been used in our analyses as described in the following sections. As can also be observed visually, in particular, C_{VD} and C_{VM} increase rapidly as the fault distance becomes smaller and as soil conditions worsen. For example, for SSTA, C_{VM} is equal to 0.4 for r=15 km and soil type A whereas it is equal to 2.3 for r=2 km and soil type E.

5. Benchmark buildings

The *superstructures* of the benchmark 3 and 8 story seismically isolated buildings, which consist of concrete moment-resisting frames formed of structural members with modulus of elasticity 32000 Mpa, are taken from Alhan and Sürmeli (2015). A typical floor plan with the cross sectional dimensions of the columns are given in Fig. 3. T-shaped interior beams have flange heights of 14 cm, web widths of 30 cm, flange widths of 100 cm, and total depths of 60 cm. L-shaped edge beams have the same dimensions as of interior T-beams but with a flange width of 70 cm. Typical
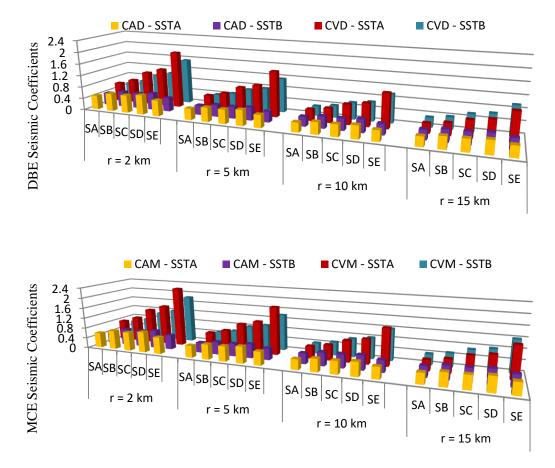

Fig. 2 Seismic coefficients for design basis earthquake (DBE) and maximum capable earthquake (MCE)

elevations of 3 and 8 story buildings, which have typical story heights of 3 m, are shown in Fig. 3.

Floor masses, which are assumed to be lumped at center of gravity (CG) of the floors, are 440 kNs²/m. The importance factor I and response modification factor R of the buildings are taken as 1.0 in the seismic analyses. The fundamental fixed-base periods are 0.41 sec and 0.74 sec for 3 and 8 story buildings, respectively in both translational directions. The superstructure modal damping ratios are assumed to be 5% for all modes.

For a comprehensive study, *nonlinear* isolation systems with different characteristic strength levels of Q/W=5%, 7.5%, and 10% in combinations with isolation periods of T_b=3.0 and 4.0 sec have been employed. The parameters used to form the isolation systems are calculated according to Section 3 and given in Table 2.

The response spectrum analysis that makes use of UBC97 design spectrum, which is constructed by using seismic coefficients employing near-source factors, requires the construction of an *equivalent linear* isolation system that are defined by parameters K_{eff} and C_{eff} (see section 3) calculated at code-prescribed (i) *design displacement* and (ii) *maximum displacement* (see Section 4).

K_{eff} and C_{eff} corresponding to a nonlinear isolation system have to be calculated at the base displacement value which would be dependent on the particular fault distance,
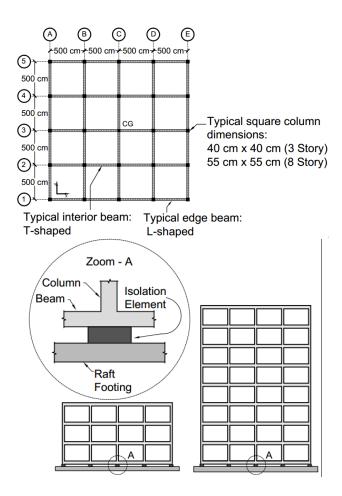

Fig. 3 Typical floor plan and elevations of benchmark seismically isolated buildings

Table 2 Non-linear isolation system parameters

Super-structure	Isolation System*	Q (kN)	α	K_2 (kN/m)	K_1 (kN/m)	F_y (kN)
3 Story	QW5Tb3	863.3	0.152	7720.2	50884.2	1017.7
	QW5Tb4	863.3	0.091	4342.6	47506.6	950.1
	QW7.5Tb3	1294.9	0.107	7720.2	72466.2	1449.3
	QW7.5Tb4	1294.9	0.063	4342.6	69088.6	1381.8
	QW10Tb3	1726.6	0.082	7720.2	94048.2	1881.0
	QW10Tb4	1726.6	0.048	4342.6	90670.6	1813.4
8 Story	QW5Tb3	1942.4	0.152	17370.5	114489.5	2289.8
	QW5Tb4	1942.4	0.091	9770.9	106889.9	2137.8
	QW7.5Tb3	2913.6	0.107	17370.5	163049.0	3261.0
	QW7.5Tb4	2913.6	0.063	9770.9	155449.4	3109.0
	QW10Tb3	3884.8	0.082	17370.5	211608.5	4232.2
	QW10Tb4	3884.8	0.048	9770.9	204008.9	4080.2

*The abbreviations indicate isolation system characteristic strength ratio Q/W and isolation period T_b. For example, QW5Tb3 is an isolation system with Q/W=5% and T_b=3 sec. The yield displacement for all isolation systems are assumed to be D_y=20 mm

the soil type, and the seismic source type in question. In order to exemplify the linearization process at *design displacement* (D_D), calculations for QW5Tb3 located at r=2 km from an SSTA seismic source and on an S_A soil is presented below:

1) Near-source factor N_v=2 (see Table 1) for SSTA and r=2 km. Correspondingly, for this case C_{VD}=0.32×N_v=0.32×2=0.64, which can also be read from Fig. 2.

2) Design displacement D_D is dependent on the effective period at design displacement (T_D) per Eq. (9). However, at the same time, T_D (i.e., T_{eff} at D_D) is calculated based on the effective stiffness per Eq. (7), which is obtained from Eq. (4) based on the design displacement D=D_D. Thus, an iterative process is required to find the set of design displacement and effective period, which satisfies all three equations concurrently.

3) Design displacement D_D is also dependent on the numerical reduction coefficient B_D per Eq. (9). The values for B_D are tabulated in UBC97 depending on the effective damping ratio β_{eff}. However, β_{eff} itself is dependent on the design displacement D=D_D per Eq. (5). Therefore, an iterative process is also required to find the set of design displacement and effective damping ratio, which satisfies all equations concurrently. Note that once β_{eff} is found, the effective viscous damping constant, which is necessary for equivalent linear modeling, can be found per Eq. (6).

4) Since design displacement D_D is dependent both on the effective period and numerical reduction coefficient for damping concurrently, the iteration processes described in steps 2 and 3 in fact have to be carried out simultaneously to yield a set of K_{eff} and C_{eff} that satisfies Eqs. (4)-(7).

Other parameters required for linearization (K_2, D_y, and Q) to be used in Eqs. (4) and (5) correspond to the specific
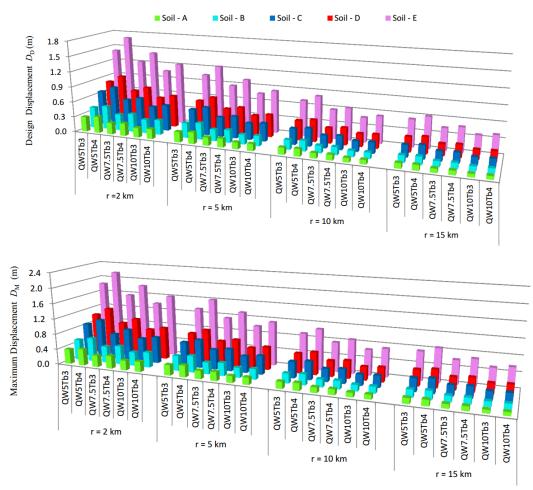
Fig. 4 UBC97 code-estimated isolation system displacements for Seismic Source Type A - SSTA

values of the nonlinear isolation system in question (see Table 2). For the example of QW5Tb3, K_2=7720.2 kN/m, Q=863.3 kN, and D_y=20 mm. Through the iteration process described above, design displacement D_D is found as 0.291 m, K_{eff}=10686.8 kN/m, β_{eff}=16.5% with corresponding B_D=1.394 (obtained from tables in UBC97). Correspondingly, C_{eff}=1427.5 kNs/m and T_{eff} (labeled as T_D for design displacement calculations) is equal to 2.55 s.

The procedure for calculating the linear isolation parameters for UBC97 prescribed *maximum displacement* (D_M) is the same as the procedure explained for design displacement (D_D) above except that Eq. (10) is used in place of Eq. (9) and the seismic coefficient C_{VM} is used instead of C_{VD}, which can be read from Fig. 2. Through iteration, for the example of QW5Tb3 discussed above, following are obtained: maximum displacement D_M=0.368 m, K_{eff}=9956.7 kN/m, β_{eff}=13.6% with corresponding B_M=1.307 (obtained from tables in UBC97). Correspondingly, C_{eff} is calculated as 1135.25 kNs/m and T_{eff} (which is labeled as T_M for maximum displacement calculations) is equal to 2.64 s.

The code-estimated values of design and maximum displacements, calculated through the iterative procedure explained above, are presented in Fig. 4 for SSTA source type (SSTB is not shown due to limited space). Fig. 4 conveniently exhibits how fast the isolation system

displacement demands, predicted by UBC97 equations employing near-source factors, increases as fault distance decreases. For example, even though both regions are located in the same first-degree seismic zone (Z4) with seismic source SSTA, for QW5Tb4 located on soil type S_E, D_M increases from 0.86 m to 2.16 m when the fault distance decreases from 15 km to 2 km (see Fig. 4). This comparison alone shows the strong influence of near-source factors. But are they necessary and if so, are they adequate? This will be discussed in detail in the following sections. It should also be noted here that the values presented in Fig. 4 are obtained via Eqs. (9) and (10) which are in effect established for single degree of freedom systems. As benchmark buildings in this study are multi degree of freedom, they do not undergo "exactly" the same amount of base displacements but values very much close to them, when analyzed via response spectrum analysis method using equivalent linear models constructed with K_{eff} and C_{eff}. In Section 7, these more accurate values are used.

6. Historical earthquakes

A total of 110 acceleration records (each with two components) from 13 historical large magnitude earthquakes are used for the bi-directional nonlinear time

Table 3 Historical earthquakes adopted from Alhan and Sürmeli (2015)

Earthquake	Date	Magnitude	Number of Records	Closest Fault Distance (km)	Seismic Source Type*	Soil Condition**
Cape Mendocino	25.04.1992	7.01	2	6.96 - 8.18	A	C
Chi-Chi	20.09.1999	7.62	33	0.32 - 13.46	A	C - D
Coalinga	02.05.1983	6.40	2	8.41	B	D
Duzce	12.11.1999	7.14	5	0.21 - 12.04	A	C - D
Erzincan	13.03.1992	6.69	1	4.38	B	D
Imperial Valley	15.10.1979	6.53	20	0.07 - 15	B	D - E
Kobe	16.01.1995	6.9	4	0.27 - 7.08	B	C - D
Kocaeli	17.08.1999	7.51	6	3.12 - 15	A	B - C - D
Landers	28.06.1992	7.28	2	2.19 - 11.03	B	C
Loma Prieta	18.10.1989	6.93	11	3.85 - 15	B	B - C - D
Nahanni	23.12.1985	6.76	2	4.93 - 9.6	B	C
Northridge	17.01.1994	6.69	18	5.19 - 13.42	B	A - C - D
Superstition Hills	24.11.1987	6.54	5	0.95 - 13.9	B	D

*Seismic source type classification is per UBC97. However, due to unavailability of slip rate data, seismic source type is identified based on the magnitude of the respective earthquake for majority of the earthquakes. Magnitude of Coalinga is very close to 6.5 and thus considered approximately as type B

**Soil classification is per UBC97. However, due to the unavailability of the standard penetration test results and undrained shear strength, the soil profile classification is based on the shear wave velocity $\bar{v}_s$ of the soil profiles, only

Table 4 Ranges of fault-distances

Ranges according to closest distance from fault, r								
Label	r1	r2	r3	r4	r5	r6	r7	r8	r9
Range (km)	0 - 1.25	1.25 - 2.50	2.50 - 3.75	3.75 - 5	5 - 6.5	6.5 - 8	8 - 10	10 - 12.5	12.5 - 15

history analyses, which are actually the records recently used by Alhan and Surmeli (2015) in investigating the necessity and the adequacy of near-source factors for *fixed-base* buildings. The records are obtained from PEER (2015). They are from the stations lying in the near-source region, i.e., from those located within 15 km range from the fault lines. The *complete details* of the records including the peak ground acceleration (PGA) and the peak ground velocity (PGV) values corresponding to the strong and the weak components, the closest fault distances, etc. are available in Alhan and Surmeli (2015). The strong components of the records are applied along the X-axis while the weak components are applied in the other orthogonal direction, i.e., along Y-axis of the benchmark buildings. Important information including the soil conditions and the seismic source types are presented in Table 3.

Very few records for A, B, and E type soils are available in the earthquake databases and thus most records used in this study are for C and D soils. Therefore, although all soil types have been considered in the analyses, we particularly focus on C and D type soils in Section 7. Also, it is important to recall that UBC 97 recommends the use of site specific spectra for structures located on E and F type soils.

Since the earthquake records have been recorded at non-uniformly varying distances of 0 to 15 km from the fault line, there was a need to define a set of ranges so that classifications of response comparisons based on fault-distances can be made more conveniently. To this end, 9 ranges of fault-distances are defined as shown in Table 4 where each range incorporates a particular number of earthquake records depending on their actual fault-distance.

7. Seismic analyses and discussion of results

Nonlinear time history analyses of the benchmark buildings with nonlinear isolation systems are conducted in 3D-BASIS (Nagarajaiah et al. 1991) while ETABS (2002) is used for linear response spectrum analyses of those with equivalent linear isolation systems (Saifullah 2015). Benchmark buildings of 3 and 8 stories in combination with six different nonlinear isolation systems (which form 12 different cases - see Table 2) are analyzed under the earthquake records described in Section 6, which required about 1300 nonlinear time history analyses. Spectrums used in linear response spectrum analyses are constructed using the concerned seismic coefficients which employ near-source factors specified in UBC97 (see Table 1 and Fig. 2). As this study focuses on large magnitude earthquakes and high seismicity zones, seismic zone Z4 (Z=0.4) and seismic source types A and B are considered. Although UBC97 allows the use of design spectra for seismically isolated buildings up to soil type D, Soil type E which requires site-specific spectra has also been included in this study for the sake of completeness of the discussions. As UBC 97 has specified near source factors for r=2, 5, 10 and 15 km and allowed linear interpolation for in-between distances, a linear interpolation of seismic response values obtained from linear response spectrum analyses at r=2, 5, 10 and 15

3 Story   **8 Story**
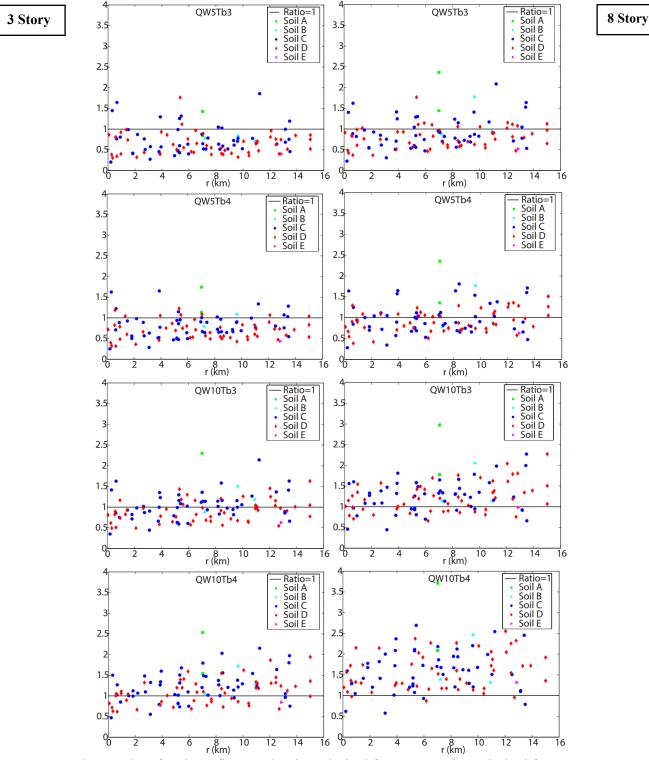

Fig. 5 Ratios of peak top floor accelerations obtained from THA to those obtained from RSA
(Results are for SSTA. Y-axis shows ratios.)

km, which required about 1000 analyses, has been carried out.

Seismic responses including base displacements, floor accelerations and inter-story drifts are included in the discussions. To see to what extent the time history analyses (THA) responses have exceeded the limit set by the response spectrum analyses (RSA) responses, the ratio of

THA responses to RSA responses is employed and results showing the number and percentage of THA responses exceeding the limit set by the RSA responses are presented in the following subsections. In the bi-directional nonlinear time history analyses, there exist two peak responses in two main horizontal directions of the structure for each analysis in terms of *design* base displacement, floor accelerations,
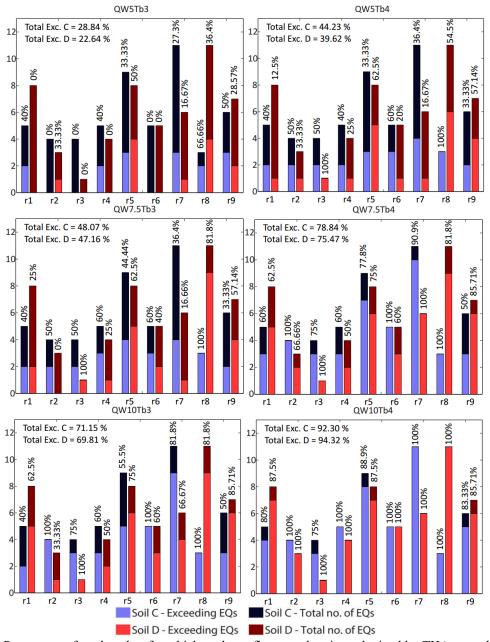
Fig. 6 Percentage of earthquakes for which peak top floor accelerations obtained by THA exceed those obtained by RSA (Results are for 8-story buildings and SSTA. Y-axis shows number of earthquakes.)

and inter-story drifts. Therefore, the larger of the peak responses obtained from THA in two main horizontal directions are compared to those obtained from RSA in the main horizontal direction. For the *maximum* base displacement response, however, the resultant peak base displacements along the most critical horizontal direction from the nonlinear time history analyses are used for comparisons. For brevity, instead of presenting results for all floors, top floor responses have been considered, which present the worst case scenario (Saifullah 2015). And due to limited space, the plots relating to seismic source type A (SSTA) and mainly those for 8-story buildings are presented here. But all results including those for 3 and 8-story buildings, seismic source types A and B, and design and maximum isolation system displacements are presented in

tables in a comprehensive and comparative manner.

7.1 Top floor acceleration

Fig. 5 shows the ratio of peak top floor acceleration responses obtained from THA to RSA for 3 and 8-story buildings. A ratio of THA/RSA=1.0 (represented by the solid line in Fig. 5) means that RSA response that is carried out under the UBC97 spectrum, which employs near-source factors, perfectly predicts the THA response. And, a ratio exceeding 1.0 means that THA response is greater than RSA response and therefore near-source factors failed short of predicting the real THA response for that case. As it can be observed from Fig. 5, there are a considerable number of cases where this ratio is greater than 1.0. And there are

Table 5 Overall results for Soil C and D combined - different isolation systems

Structure	Isolation System	Top Floor Acceleration		Inter-Story Drift		Design Base Displacement		Maximum Resultant Base Displacement	
		No. of Earthquakes Exceeding	Percentage of Earthquakes Exceeding (%)	No. of Earthquakes Exceeding	Percentage of Earthquakes Exceeding (%)	No. of Earthquakes Exceeding	Percentage of Earthquakes Exceeding (%)	No. of Earthquakes Exceeding	Percentage of Earthquakes Exceeding (%)
SSTA									
3 Story	QW5Tb3	11	10.48	10	9.52	14	13.33	7	6.67
	QW5Tb4	18	17.14	15	14.29	13	12.38	6	5.71
	QW7.5Tb3	23	21.90	20	19.05	14	13.33	8	7.62
	QW7.5Tb4	44	41.90	36	34.29	12	11.43	5	4.76
	QW10Tb3	41	39.05	34	32.38	13	12.38	9	8.57
	QW10Tb4	72	68.57	66	62.86	16	15.24	6	5.71
8 Story	QW5Tb3	27	25.71	22	20.95	13	12.38	7	6.67
	QW5Tb4	44	41.90	30	28.57	11	10.48	6	5.71
	QW7.5Tb3	50	47.62	37	35.24	13	12.38	6	5.71
	QW7.5Tb4	81	77.14	72	68.57	9	8.57	7	6.67
	QW10Tb3	74	70.48	68	64.76	11	10.48	8	7.62
	QW10Tb4	98	93.33	94	89.52	13	12.38	7	6.67
SSTB									
3 Story	QW5Tb3	18	30.51	18	30.51	16	27.12	9	15.25
	QW5Tb4	23	38.98	20	33.90	15	25.42	9	15.25
	QW7.5Tb3	32	54.24	30	50.85	19	32.20	12	20.34
	QW7.5Tb4	40	67.80	40	67.80	20	33.90	10	16.95
	QW10Tb3	45	76.27	43	72.88	18	30.51	11	18.64
	QW10Tb4	48	81.36	48	81.36	22	37.29	11	18.64
8 Story	QW5Tb3	32	54.24	27	45.76	15	25.42	9	15.25
	QW5Tb4	39	66.10	32	54.24	12	20.34	9	15.25
	QW7.5Tb3	45	76.27	38	64.41	17	28.81	12	20.34
	QW7.5Tb4	56	94.92	55	93.22	16	27.12	9	15.25
	QW10Tb3	55	93.22	52	88.14	16	27.12	11	18.64
	QW10Tb4	59	100.0	57	96.61	19	32.20	11	18.64

Table 6 Overall results for Soil C and D combined - all isolation systems included

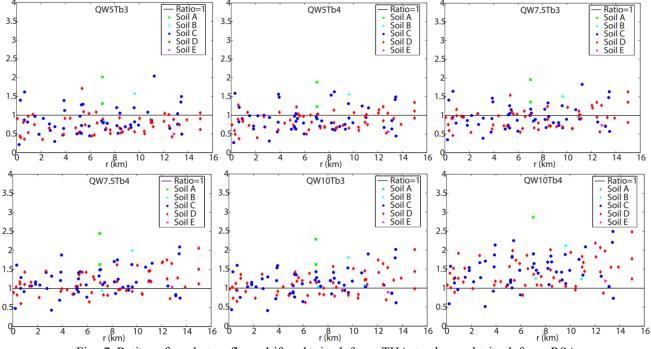| Seismic Source Type	Structure	Closes Fault Distance, r (km)	Top Floor Acceleration	Inter-Story Drift	Base Displacement	Maximum Resultant Base Displacement
			Percentage of Earthquakes Exceeding	Percentage of Earthquakes Exceeding	Percentage of Earthquakes Exceeding	Percentage of Earthquakes Exceeding
SSTA	3 Story	0 - 5	22.55	19.61	15.20	9.31
		5 - 10	35.61	32.20	11.74	4.92
		10 - 15	42.59	34.57	12.35	5.56
	8 Story	0 - 5	51.47	42.16	15.20	10.29
		5 - 10	59.85	52.65	9.09	4.17
		10 - 15	68.52	60.49	9.26	5.56
SSTB	3 Story	0 - 5	56.86	55.88	47.06	23.53
		5 - 10	67.39	64.49	41.30	27.54
		10 - 15	48.25	46.49	4.39	0
	8 Story	0 - 5	75.49	71.57	45.10	22.55
		5 - 10	84.06	76.09	32.61	27.54
		10 - 15	81.58	72.81	3.510	0

Fig. 7 Ratios of peak top floor drifts obtained from THA to those obtained from RSA
(Results are for 8-story buildings and SSTA. Y-axis shows ratios.)

quite a few cases where THA response is as much as 2.5 times RSA response, showing that near-source factors fail short by a large margin in terms of floor acceleration responses. It is also observed from Fig. 5 and from Tables 5 and 6 that the percentage of top floor acceleration responses obtained by THA exceeding RSA is consistently higher for 8-story buildings compared to 3-story buildings for all types of isolation systems considered. Additionally, it is clear that the number of failing cases increases with increasing isolation system characteristic strength level and increasing

isolation period. Fig. 6 gives the details of the results obtained for soil types C and D for 8-story buildings in case of SSTA earthquakes. It is observed from Fig. 6 that for 8-story buildings, the worst case appears to be QW10Tb4 where 92.3% of the cases for Soil type C exceeded the THA/RSA=1.0 limit and 94.32% for Soil type D. The aforementioned trends are similar for seismic source type B for which the 8-story building with QW10Tb4 is again the worst case (see Table 5). The results clearly indicate that the near-source factors are highly unconservative from top floor
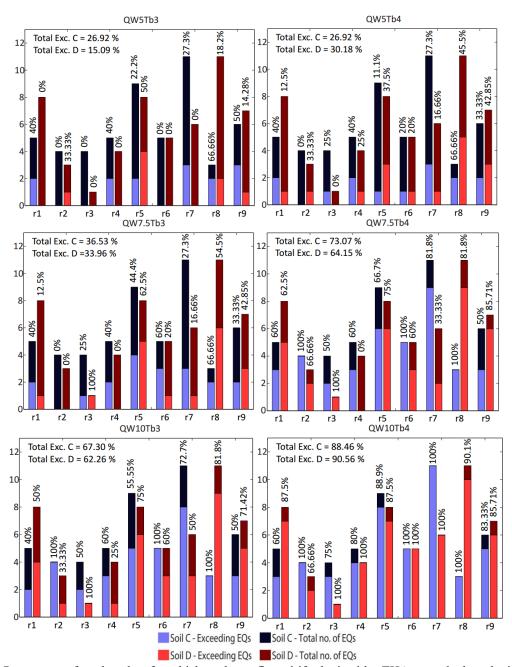
Fig. 8 Percentage of earthquakes for which peak top floor drift obtained by THA exceeds that obtained by RSA (Results are for 8-story buildings and Seismic Source Type A. Y-axis shows number of earthquakes.)

acceleration viewpoint.

7.2 Inter-story drift

Just like the acceleration responses, for inter-story drifts, increasing isolation period and increasing isolation system characteristic strength resulted in more number of earthquakes exceeding the limit THA/RSA=1.0 as depicted in Figs. 7 and 8. For the 8-story building and considering SSTA, the highest percentages of exceedance are 88.46% on Soil type C and 90.56% on Soil type D, which are in fact observed for QW10Tb4 (Fig. 8 and Table 5). Thus, QW10Tb4 again represents the worst case scenario where 62.86% and 89.52% of earthquakes (occurring on C and D type soils combined) exceeded THA/RSA=1.0 limit for 3 and 8-story building, respectively (see Table 5 - SSTA). In terms of inter-story drift responses, THA/RSA ratios are concentrated between 1 and 2.5 for the worst case i.e. QW10Tb4 (Fig. 7). Similar to the acceleration responses, the increase in number of stories in the superstructure results in more number of earthquakes exceeding the THA/RSA=1.0 limit (see Tables 5 and 6). And the results for SSTB follow the same trend as SSTA. The overall exceedance for SSTB can reach 96.61 %, which is realized for 8-story building with QW10Tb4 (see Table 5). These results clearly demonstrate the shortcomings and unconservativeness of near-source factors from inter-story drift viewpoint.
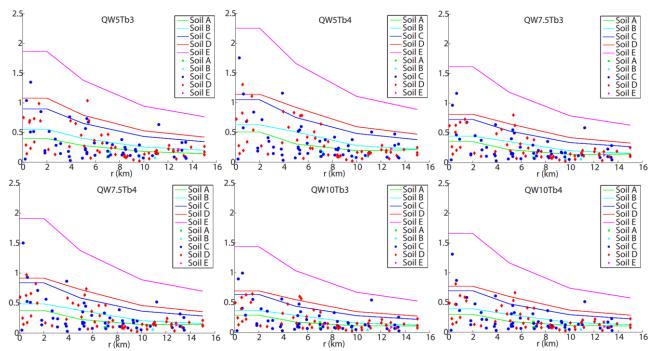
Fig. 9 Maximum base displacement, D_M (Results are for 8-story buildings and SSTA. Y-axis shows displacement in meters. Points on the plots represent THA responses while lines represent RSA responses)
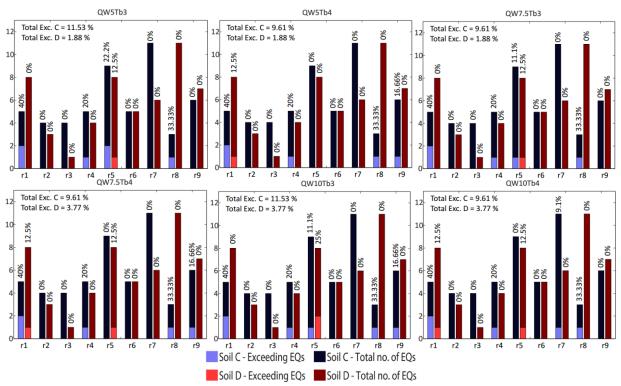

Fig. 10 Percentage of earthquakes for which maximum base displacement D_M obtained by THA exceeds that obtained by RSA (Results are for 8-story buildings and Seismic Source Type A. Y-axis shows number of earthquakes.)

7.3 Maximum base displacement

Compared to superstructure responses, much less exceedance is observed in terms of maximum resultant base displacements, for SSTA (Figs. 9, 10 and Tables 5, 6). And the maximum exceedance value (considering C and D type soils combined) is 8.57%, which is observed for 3 story building with QW10Tb3 (see Table 5). Unlike superstructure responses, no particular increasing or decreasing trend of exceedance is observed depending on the isolation period or the isolation system characteristic strength. The low values of exceedance indicate that near-

source factors, for SSTA, are fairly conservative for maximum base displacement. For SSTB, trends are similar to SSTA but relatively more exceedance is observed compared to SSTA. The overall exceedance for SSTB can reach 20.34%, which is realized for QW7.5Tb3 (Table 5). Relatively higher values of exceedance for SSTB indicate the relative unconservativeness of near-source factors for SSTB compared to SSTA.

7.4 Design base displacement

For design displacement of isolation system, in case of SSTA, it is observed that exceedances are typically more than 10% and less than 15%, with a maximum value of 15.24% seen in the case of QW10Tb4 for 3-story building (Table 5). These values indicate that near-source factors in case of SSTA are somewhat conservative for design displacements. For SSTB, much more number of earthquakes exceeds the limit THA/RSA=1.0. In this case, the exceedance can reach as much as 37.2% for 3-story building with QW10Tb4 (Table 5 - SSTB). Likewise maximum displacement, no particular increasing or decreasing trend of exceedance is observed, with increasing isolation period or isolation system characteristic strength, for both SSTA and SSTB. Higher values of exceedance for SSTB illustrate the inadequacy of near-source factors for design base displacement for SSTB.

8. Conclusions

The 1997 Uniform Building Code has specified near-source factors that scale up the design spectrum depending on the closest distance to the fault, the soil type at the site, and the properties of the seismic source. These factors are expected to account for the so-called near-fault effects, which may cause increased seismic demands in base-isolated buildings. Although UBC97 has been superseded by the 2015 International Building Code in the U.S.A., which makes use of detailed spectral maps instead of near-source factors, UBC97 near-source factors are still frequently used in the designs of seismically isolated buildings in the countries with seismic codes that do not contain detailed spectral maps. Just recently, Alhan and Sürmeli (2015) investigated the adequacy and necessity of UBC97 near-source factors for the conventional fixed-base buildings and concluded that these factors are utterly necessary but the current values are inadequate for fixed-base buildings. And in this study, the necessity and the adequacy of near-source factors defined in UBC97 for seismically isolated buildings has been explored by comparing seismic responses of benchmark 3 and 8-story base-isolated buildings obtained via nonlinear time history analyses using a large number of historical earthquakes with those obtained from linear spectral analyses using the amplified spectrums established through UBC97 near-source factors.

Based on the observations regarding the time history analyses (THA) responses exceeding the response spectrum analyses (RSA) responses, the conclusions are as under:

1. For seismic source type A, the near-source factors appear to be fairly conservative for design base displacement and maximum base displacement as most of the exceedance for both lies around 10%. For seismic source type B, the near-source factors are not as conservative for design base displacement and maximum base displacement as the exceedance value can reach up to 37% for the former and 20% for the latter. Thus, a moderate increase in near-source factors for seismic source type B could be considered in order to increase the safety margin.

2. No specific general trend, depending on the isolation period or the isolation system characteristic strength, is observed in terms of the conservativeness of near-source factors regarding base displacement.

3. The near-source factors for both seismic source types A and B are very unconservative in terms of superstructure responses, as the exceedance can reach more than 90% for both of them. Thus, it is recommended that extra amplification factors (in addition to near-source factors) be introduced for superstructure responses.

4. The qualitative trends obtained via the parametric analyses carried here suggest that the unconservativeness of near-source factors, in terms of floor accelerations and inter-story drifts, becomes more critical as (i) the isolation period, (ii) the isolation system characteristic strength, and (iii) flexibility of the superstructure increases.

References

Alhan, C. and Gavin, H. (2004), "A parametric study of linear and non-linear passively damped seismic isolation systems for buildings", *Eng. Struct*., **26**(4), 485-497.

Alhan, C., Gavin, H. and Aldemir, U. (2006), "Optimal control: basis for performance comparison of passive and semiactive isolation systems", *J. Struct. Eng.*, **132**(7), 705-713.

Alhan, C. and Öncü-Davas (2016), "Performance limits of seismically isolated buildings under near-field earthquakes", *Eng. Struct.*, **116**, 83-94

Alhan, C. and Özgür, M. (2015), "Seismic responses of base-isolated buildings: efficacy of equivalent linear modeling under near-fault earthquakes", *Smart Struct. Syst.*, **15**(6), 1436-1461.

Alhan, C. and Sürmeli, M. (2015), "The necessity and the adequacy of near-source factors for not-so-tall fixed-base buildings", *Earthq. Eng. Eng. Vib.*, **14**(1), 13-26.

Asher, J.W., Young, R.P. and Ewing, R.D. (1996), "Seismic isolation design of the San Bernardino County Medical Center replacement project", *Struct. Des. Tall Build.*, **5**(4), 265-279.

Becker, T.C., Yamamoto, S., Hamaguchi, H., Higashino, M. and Nakashima, M. (2015), "Application of isolation to high-rise buildings: A Japanese design case study through a U.S. design code lens", *Earthq. Spectra*, **31**(3), 1451-1470.

Bolt, B.A. (2004), *Engineering seismology, in Earthquake Engineering from Engineering Seismology to Performance-Based Engineering*, Eds., Bozorgnia Y and Bertero VV, CRC Press.

Bolt, B.A. and Abrahamson, N.A. (2003), *Estimation of strong seismic ground motions, in International Handbook of Earthquake and Engineering Seismology Part B*, Eds., Lee WHK, Kanamori H, Jennings PC, and Kisslinger, C, Book Series: International Geophysics Series, 81B, Academic Press Elsevier Science.

Building Code of Pakistan - Seismic Provisions (2007), Ministry of Housing and Works, Government of Pakistan.

Chavez, J.W. (2012), "Overview of the current seismic codes in Central and South America", *Bull. IISEE*, **46**, 153-160.

Constantinou, M.C. and Symans, M.D. (1992), "Experimental and analytical investigation of seismic response of structures with supplemental fluid viscous dampers", Technical Report NCEER-92-0032, National Center for Earthquake Engineering Research, State University of New York at Buffalo.

Dan, M., Ishizawa, Y., Tanaka, S., Nakahara, S., Wakayama, S. and Kohiyama, M. (2015), "Vibration characteristics change of a base-isolated building with semi-active dampers before, during, and after the 2011 Great East Japan earthquake", *Earthq. Struct.*, **8**(4), 889-913.

ETABS (2002), "Integrated building design software", *Computers and Structures Inc.* Berkeley, USA.

Gavin, H., Alhan, C. and Oka, N. (2003), "Fault tolerance of semiactive seismic isolation", *J. Struct. Eng.*, **129**(7), 922-932.

Hall, J.F., Heaton, T.H., Halling, M.W. and Wald, D.J. (1995), "Near-source ground motion and its effects on flexible buildings", *Earthq. Spectra*, **11**(4), 569-605.

Hall, J.F. and Ryan, K.L. (2000), "Isolated buildings and the 1997 UBC near-source factors", *Earthq. Spectra*, **16**(2), 393-411.

Heaton, T.H., Hall, J.F., Wald, D.J. and Halling, M.W. (1995), "Response of high-rise and base-isolated buildings to a hypothetical *M(W)* 7.0 blind thrust earthquake", *Science*, **267**(5195), 206-211.

Hoseini Vaez, S.R., Naderpour, H. and Barros, R.C. (2014), "Influence of equivalent pulses of near fault ground motions on base-isolated RC structures", *Proceedings of the 9th International Conference on Structural Dynamics*, *EURODYN*, 30 June-2 July, Porto.

Hussain, S., Lee, D. and Retamal, E. (1998), "Viscous damping for base isolated structures", Taylor Devices Inc. North Tonawanda, NY.

Inaudi, J.A. and Kelly, J.M. (1993), "Hybrid isolation systems for equipment protection", *Earthq. Eng. Struct. Dyn.*, **22**(4), 297-313.

Indian Standard - Criteria for Earthquake Resistant Design of Structures (2002), IS 1893 (Part 1), Fifth Revision, Bureau of Indian Standards.

Iranian Code of Practice for Seismic Resistant Design of Buildings (2007), Standard No. 2800, Third Edition, Publication No. S-465, Permanent Committee for Revising the Iranian Code of Practice for Seismic Resistant Design of Buildings.

Jangid, R.S. and Kelly, J.M. (2001), "Base isolation for near-fault motions", *Earthq. Eng. Struct. Dyn.*, **30**(5), 691-707.

Kani, N. (2011), "Recent Trends of Seismically Isolated Structures in Japan", *The Japan Society for Seismic Isolation*, Tokyo, Japan.

Kelly, J.M. (1999), "The role of damping in seismic isolation", *Earthq. Eng. Struct. Dyn.*, **28**(1), 3-20.

Komuro, T., Nishikawa, Y., Kimura, Y. and Isshiki, Y. (2005), "Development and realization of base isolation system for high-rise buildings", *J. Adv. Concrete Technol.*, **3**(2), 233-239.

Lu, L.-Y., Lin, C.-C. and Lin, G.-L. (2013), "Experimental evaluation of supplemental viscous damping for a sliding isolation system under pulse-like base excitations", *J. Sound Vib.*, **332**(8), 1982-1999.

Lu, X., Wang, D. and Wang, S. (2016), "Investigation of the seismic response of high-rise buildings supported on tension-resistant elastomeric isolation bearings", *Earthq. Eng. Struct. Dyn.*, doi: 10.1002/eqe/2755.

Lu, Y. and Panagiotou, M. (2015), "Earthquake damage-resistant tall buildings at near fault regions using base isolation and rocking core walls", *Struct. Congress*, 1266-1277.

Makris, N. (1997), "Rigidity-Plasticity-Viscosity: Can electrorheological dampers protect base-isolated structures from near-source ground motions?", *Earthq. Eng. Struct. Dyn.*, **26**(5),

571-591.

Makris, N. and Chang, S.P. (2000), "Effect of viscous, viscoplastic and friction damping on the response of seismic isolated structures", *Earthq. Eng. Struct. Dyn.*, **29**(1), 85-107.

Martelli, A., Clemente, P., De Stefano, A., Forni, M. and Salvatori, A. (2014), *Recent development and application of seismic isolation and energy dissipation and conditions for their correct use, Perspectives on European Engineering and Seismology*, Ed., Atilla Ansal, Book Series: Geotechnical, Geological and Earthquake Engineering, **1**, 449-488, Springer.

Matsagar, V.A. and Jangid, R.S. (2004), "Influence of isolator characteristics on the response of base-isolated structures", *Eng. Struct.*, **26**(12), 1735-1749.

Mazza, F. and Vulcano, A. (2009), "Nonlinear response of RC framed buildings with isolation and supplemental damping at the base subjected to near-field earthquakes", *J. Earthq. Eng.*, **13**(5), 690-715.

Naderzadeh, A. (2009), "Application of seismic base isolation technology in Iran", MENSHIN, **63**, 40-47.

Naeim, F. and Kelly, J.M. (1999), *Design of seismic isolated structures: from theory to practice, mechanical characteristics and modeling of isolators*, New York, Wiley.

Nagarajaiah, S., Reinhorn, A.M. and Constantinou, M.C. (1991), "Nonlinear dynamic analysis of three-dimensional base isolated structures: Part II", Technical Report NCEER-91-0005, *National Center for Earthquake Engineering, State University of New York at Buffalo*, New York, USA.

Nitta, Y., Nishitani, A. and Spencer Jr., B.F. (2006), "Semiactive control strategy for smart base isolation utilizing absolute acceleration information", *Struct. Control Hlth. Monit.*, **13**(2-3), 649-659.

PEER (2015), "Strong ground motion database", *Pacific Earthquake Engineering Research Center*, University of California, Berkeley, USA. http://ngawest2.berkeley.edu/site

Providakis, C.P. (2008), "Effect of LRB isolators and supplemental viscous dampers on seismic isolated buildings under near-fault excitations", *Eng. Struct.*, **30**(5), 1187-1198.

Providakis, C.P. (2009), "Effect of supplemental damping on LRB and FPS seismic isolators under near-fault ground motions", *Soil Dyn. Earthq. Eng.*, **29**(1), 80-90.

Ramallo, J.C., Johnson, E.A. and Spencer Jr., B.F. (2002), ""Smart" base isolation systems", *J. Eng. Mech.*, **128**(10), 1088-1099.

Ribakov, Y. (2010), "Reduction of structural response to near fault earthquakes by seismic isolation columns and variable friction dampers", *Earthq. Eng. Eng. Vib.*, **9**(1), 113-122.

Ribakov, Y. (2011), "Base-isolated structures with selective controlled semi-active friction dampers", *Struct. Des. Tall Spec. Build.*, **20**(7), 757-766.

Ribakov, Y. and Agranovich, G. (2008a), "Using hybrid isolation systems with friction dampers for seismic protection of structures", ENOC, Saint Petersburg, Russia.

Ribakov, Y., Blostotsky, B. and Iskhakov, I. (2006), "Theoretical model and laboratory tests of variable friction damper", *Eur. Earthq. Eng.*, **20**(1), 43-47.

Ribakov, Y. and Iskhakov, I. (2008), "Experimental methods for selecting base isolation parameters for public buildings", *Open Constr. Build. Technol. J.*, **2**, 1-6.

Saifullah, M.K. (2015), "The necessity and the adequacy of near-source factors for seismically isolated buildings", *Master Thesis, Istanbul University*, Istanbul, Turkey.

Symans, M.D. and Constantinou, M.C. (1999), "Semi-active control systems for seismic protection of structures: A state-of-the-art review", *Eng. Struct.*, **21**(6), 469-487.

Taylor, D.P. (1996), "Fluid dampers for application of seismic energy dissipation and seismic isolation", Eleventh World Conference on Earthquake Engineering, Paper No. 798,

Acapulco, Mexico, June 23-28.

TEC07 (2007), "Turkish Earthquake Code: Regulations on Structures Constructed in Disaster Regions", Ministry of Public Works and Settlement, Ankara, Turkey.

Tsang, H.-H., Lo, S.H., Xu, X. and Sheikh, M.N. (2012), "Seismic isolation for low-to-medium-rise buildings using granulated rubber-soil mixtures: numerical study", *Earthq. Eng. Struct. Dyn.*, **41**(14), 2009-2024.

UBC97 (1997), Uniform Building Code. International code of building officials (ICBO), California, USA.

Wolff, E.D., Ipek, C., Constantinou, M.C. and Tapan, M. (2015), "Effect of viscous damping devices on the response of seismically isolated structures", *Earthq. Eng. Struct. Dyn.*, **44**(2), 185-198.

Yang, J.N. and Agarwal, A.K. (2002), "Semi-Active hybrid control systems for nonlinear buildings against near-field earthquakes", *Eng. Struct.*, **24**(3), 271-280.

CC